Surv Geophys (2014) 35:101–122
DOI 10.1007/s10712-013-9236-0

Exploring for Geothermal Resources with Electromagnetic Methods

Gerard Muñoz

Received: 1 October 2012 / Accepted: 22 April 2013 / Published online: 17 May 2013

Abstract Electrical conductivity of the subsurface is known to be a crucial parameter for the characterization of geothermal settings. Geothermal systems, composed by a system of faults and/or fractures filled with conducting geothermal fluids and altered rocks, are ideal targets for electromagnetic (EM) methods, which have become the industry standard for exploration of geothermal systems. This review paper presents an update of the state-of-the-art geothermal exploration using EM methods. Several examples of high-enthalpy geothermal systems as well as non-volcanic systems are presented showing the successful application of EM for geothermal exploration but at the same time highlighting the importance of the development of conceptual models in order to avoid falling into interpretation pitfalls. The integration of independent data is key in order to obtain a better understanding of the geothermal system as a whole, which is the ultimate goal of exploration.

Keywords Geothermics · Electromagnetics · Electrical resistivity · Exploration

1 Introduction

Geothermal energy is an attractive renewable energy which is becoming an important contributor to the energy mix. In 2008, its power production exceeded that of solar photovoltaics more than three times (Rybach 2010). However, contrary to other renewable energy sources like solar or wind energy, which exhibit exponential growths, geothermal energy has been experiencing a linear growth in the last years (Rybach 2010; Bertani 2010). Some optimistic forecasts also point to an exponential growth for geothermal energy (Bertani 2010), especially based on technologic developments like enhanced (or engineered) geothermal systems (EGS) (Rybach 2010) which are viewed by some studies

Electronic supplementary material The online version of this article (doi:10.1007/s10712-013-9236-0) contains supplementary material, which is available to authorized users.

G. Muñoz (✉)
German Research Centre for Geosciences GFZ, Telegrafenberg, 14473 Potsdam, Germany
e-mail: gmunoz@gfz-potsdam.de

as the future of geothermal energy utilization (Tester et al. 2006). EGS are universally deployable, as no special geological settings are required but generally involve deeper targets and therefore highlight the need for reliable exploration techniques. Exploration for geothermal energy is also of great importance in conventional geothermal systems in order to improve its economic viability (Barbier 2002). Over the last years, there has been an important increase in the use and development of several exploration methods for geothermal resources, seismic as well as electromagnetic (EM); but while the former (like repeated 3D surface seismic, surface-to-borehole vertical seismic and borehole-to-borehole cross-well seismic profiling) have not always led to better understanding of the geothermal systems, the latter have become very popular due to improved equipment, methodologies and processing and modelling software (Spichak and Manzella 2009).

The electrical conductivity of the subsurface is known to be a crucial parameter for the characterization of geothermal settings. Geothermal systems are in general composed by a region or system of faults and fractures filled with geothermal fluids, which can have high concentrations of dissolved salts, thus resulting in conducting electrolytes in a rock matrix. Both fluid and matrix (to a lesser extent) conductivities depend on temperature, and the geothermal system exhibits, generally, higher conductivity values than the host rocks. Clay mineral alterations resulting from the hydrothermal processes that take place in geothermal systems also have a high conductivity signature. This makes geothermal systems ideal targets for EM methods, which have become the industry standard for exploration of geothermal systems in many countries. The relatively easy to identify low resistivity zones produced by brines and clays that cap a geothermal system (Wright et al. 1985) represent attractive targets for exploration; however, this "anomaly hunting" (Cumming 2009) can sometimes be misleading; clay caps produce high conductivity anomalies but the opposite is not true, not all conductive anomalies are clay caps.

In recent years, many papers have been published about the use of electromagnetic methods for exploration of geothermal zones, including some review papers (Pellerin et al. 1996; Meju 2002; Spichak and Manzella 2009). In this review paper, I will try to present an update of the state-of-the-art geothermal exploration using EM methods. First, I will present the conceptual conductivity models of classical convective hydrothermal systems briefly summarizing the causes of the observed conductivities in geothermal systems and will introduce other kinds of possible geothermal targets. I will present a number of examples of use of EM methods for imaging of geothermal targets, both in classical "clay cap" systems and in other geological settings (e.g., sedimentary basins). I will focus on magnetotelluric (MT) techniques, as it is the only method to reliably reach depths of several kilometres needed for some geothermal targets, but I will not forget other EM methods and I will highlight the importance of incorporating as much additional data (geological, geophysical, geochemical,…) as possible in order to obtain a better understanding of the geothermal system as a whole, which is the ultimate goal of exploration.

2 Conceptual Model

Geothermal resources, understood as systems that store natural heat in rock and fluids within the Earth, can be divided into different types according to the temperature and the nature of the reservoir. A primary division of the geothermal systems can be made according to whether they are related to emplacement of magma or not. Magmatic geothermal systems include convective hydrothermal systems (water or steam dominated), hot dry rock and partial melt systems, while non-volcanic resources are usually related to hot fluids in sedimentary or crystalline reservoirs (Meju 2002). Enhanced (or engineered) geothermal systems (EGS) are geothermal resources with low permeability and/or porosity and high temperature which need artificial stimulation of the fracture system to enhance the fluid circulation. On the other end of the spectrum are supercritical systems, where fluids are in supercritical conditions and for which the efficiency of power generation would be very high.

Hydrothermal systems represent the most common type of geothermal reservoir (in terms of exploitation) and most of the literature on exploration for geothermal resources is related to hydrothermal systems. An ideal hydrothermal system consists, conceptually, of a heat source, some sort of groundwater system to transport and sometimes store the heat (reservoir) and a confining impermeable structure (cap). Geothermal fluids have salts dissolved in high concentrations which provide conducting electrolytes within a rock matrix. Both the conductivities of the fluids and the rock matrix are dependent on temperature in a way that causes a large reduction in the bulk resistivity with increasing temperature. The confining cap for most of the hydrothermal systems is produced by prolonged reactions of the rocks with the thermal fluids, which produce a clay alteration layer over a wide temperature range from under 100 °C to over 200 °C (Caldwell et al. 1986; Essene and Peacor 1995). At lower temperatures (70–150 °C), the clay cap is mainly characterized by smectite. At higher temperatures, illite (in acidic rocks) and/or chlorite (more abundant in basaltic rocks) become interlayered with smectite, forming a mixed layer with increasing proportions, especially above 180 °C. At temperatures over 220–240 °C, alteration is mainly in form of chlorite and epidote minerals, which show a higher resistivity signature than its lower temperature counterparts. The low temperature (<150 °C) alteration species (illite–smectite) are significantly more conductive than the higher temperature (chlorite–epidote) species (Björnsson et al. 1986). Smectites and illites have loosely bound cations that make these minerals electrically conductive, whereas in the chlorites and epidotes, all ions are bound in the crystal lattice and are, therefore, more resistive (Deer et al. 1962). Thus, an increase in resistivity beneath a highly conductive surficial layer (clay cap), reflecting an increase in temperature with depth, is a common signature of high-temperature geothermal systems. For a compact but comprehensive review on the causes of enhanced electrical conductivity in geothermal systems see Ussher et al. (2000) and references therein.

The strong link between electrical resistivity and clay minerals and therefore temperature allows using the resistivity structure as distinguishing mark for high-temperature areas. Alteration, however, is generally unaffected by subsequent cooling, and in most cases, the resistivity structure can be regarded as a “maximum thermometer” (Árnason et al. 2010). In a simple hydrothermal context, the geothermal system can be conceptualized with the model of Fig. 1a. In a more generalized context, the upflow and outflow areas can affect the geometry of the low resistivity zone. The upflow area is a zone in the reservoir where the fluid flow is predominantly vertical and generally the temperature increases with depth. In upflow areas, the base of the conductive clay cap is often elevated because of the relative increase in higher resistivity minerals in the mixed layer with temperature (i.e. depth). In cooler outflow areas, where the flow is predominantly horizontal and temperature decreases with depth below the main outflow zone, the base of the clay cap can come closer to the surface and the geometry of the high conductivity anomaly can be asymmetric and not centred on the reservoir (Anderson et al. 2000). An example of such a generalized geothermal system is shown in Fig. 1b. In some cases at high-temperature volcanic-associated geothermal systems, the clay cap may even be absent. In many high-temperature liquid-dominated geothermal systems, the fluid, which is dominantly meteoric, is not re-circulated but after being heated at depth, it rises by convection to near-surface depths, where it is entrained into the overall pattern of groundwater flow or discharged joining the surface drainage (Meju 2002), like in many liquid-dominated geothermal systems in New Zealand (Bibby et al. 1995). The most favourable conditions for high-temperature systems that can be used for electricity production usually occur when magma intrudes into shallow crustal levels (<10 km depth) and hydrothermal convective fluid flow can take place above the intrusion body.

Non-magmatic geothermal systems, on the other hand, exhibit a much greater variation in geometry, and it is generally not possible to construct a conceptual model encompassing the whole range of non-magmatic geothermal systems. The exact nature of conductive anomalies (if present) can vary greatly between different geothermal systems but, in general, it is related to electrolytic conduction in saline fluids. Geothermal fluids tend to have high concentrations of dissolved salts, and their conductivity increases with temperature (Ucok et al. 1980). For non-magmatic geothermal systems, imaging the electrical conductivity distribution helps locating deep aquifers that can act as reservoirs and fluid pathways. In EGS, however, low natural permeability and depth of the system can produce relatively small and badly connected targets which might be difficult to image with electromagnetic methods. In these cases, EM methods can be very helpful in monitoring the engineering process by providing images before, during and after stimulation activities and estimating the enhancement in permeability achieved. In geothermal systems where saline fluids are key players, its electrical properties can greatly vary depending on whether faults and fractures constitute pathways that can enhance fluid (and heat) circulation or whether they represent barriers impeding fluid circulation (Ritter et al. 2005).

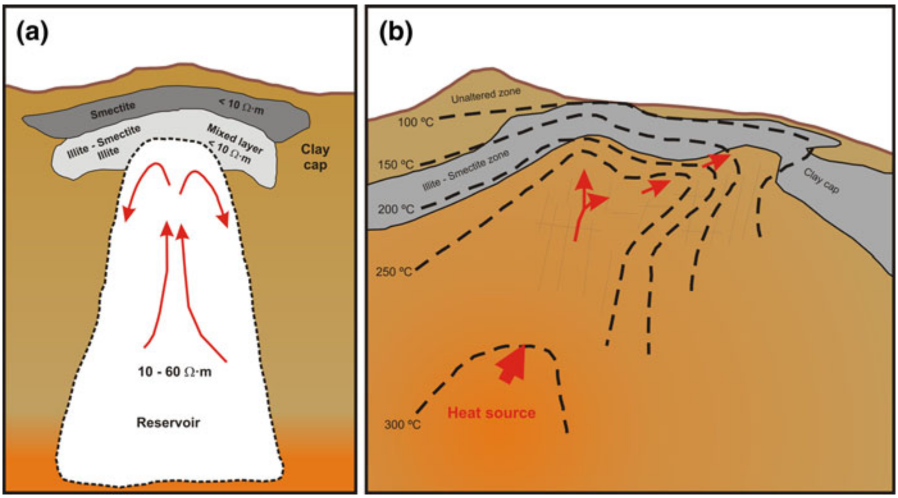

Fig. 1 **a** Conceptual model of a geothermal system in a simple hydrothermal context. Clay alteration layer shows lower resistivity than the surrounding background rocks (redrawn from Pellerin et al. 1996). **b** Conceptual model of a generalized geothermal system (redrawn from Cumming 2009). The upflow and outflow areas affect the geometry of the conductive clay cap and cause the anomaly not to be centred on the reservoir

3 High-Enthalpy Geothermal Systems

High-enthalpy geothermal systems (defined as geothermal systems with temperature above 150–200 °C; for example, Muffler and Cataldi 1978; Benderitter and Cormy 1990) are most commonly found in tectonically active regions, such as plate boundaries, rift zones and above hot spots, or in young volcanic regions, where the total thermodynamic energy is high enough to generate such temperatures. High-enthalpy geothermal systems are the most likely systems to be described by the conceptual model introduced in the previous section (Fig. 1). This kind of electrical resistivity distributions (conductive clay cap overlying a more resistive reservoir) has been observed using a variety of electromagnetic methods in many regions in the world. Next, I will summarize the most significant findings at some exemplary geothermal areas (see location in Online Resource 1). However, these are not by far the only possible examples. Similar high-enthalpy geothermal systems have been found for instance in Central America (e.g., El Salvador—Romo et al. 1997), Africa (e.g., Ethiopia—Abiye and Haile 2008; Djibouti—Árnason and Flovenz 1998; Kenya—Mwangi 2012), Indonesia (e.g., Sibayak in Sumatra—Mulyadi 2000; Daud et al. 2001; Bajawa in Flores—Uchida et al. 2002; Kamojang in Java and Lahendong in Sulawesi—Raharjo et al. 2010), Japan (e.g., Sumikawa—Uchida 1995; Muraoka et al. 1998; Uchida et al. 2000; Yamane et al. 2000; Mt. Aso—Asaue et al. 2005; Minamikayabe—Spichak 2005; Ogiri—Uchida 2005; Yanaizu-Nishiyama—Uchida et al. 2010), Greece (e.g., Lagios et al. 1998), Turkey (e.g., Burçak et al. 2005; Kuyumcu et al. 2011) or Russia (e.g., Spichak et al. 2007; Nurmukhamedov et al. 2010).

3.1 Taupo Volcanic Zone (New Zealand)

The Taupo Volcanic Zone (TVZ) is a region of extension and rhyolite volcanism associated with the subduction of the Pacific plate beneath the New Zealand's North Island. Associated with the active volcanism are more than 20 high-temperature geothermal systems with a total heat output of more than 4,000 MW (Bibby et al. 1995). Early exploration of the TVZ represents perhaps the most successful application of electrical resistivity techniques for delineating geothermal systems (Bibby et al. 2005). Electrical resistivity maps (e.g., Bibby 1988; Stagpoole and Bibby 1998) show that all known geothermal systems within the TVZ are associated with low resistivity zones, while the surrounding volcanic rocks are cold water saturated and more resistive. A characteristic resistivity increase beneath the highly conductive surficial layer is seen within most geothermal systems of the TVZ and is clearly demonstrated by the Schlumberger mapping (Bibby 1988). Thus, all known geothermal systems in the TVZ comply with the classical hydrothermal conceptual model of Fig. 1a. The converse, however, is not true, and not all low resistivity zones correspond with active hydrothermal systems.

The whole Taupo Volcanic Zone has been extensively studied using electromagnetic methods (see, e.g., Bibby et al. 1995, 2002; Ogawa et al. 1999; Heise et al. 2007; Bertrand et al. 2012 and references therein) among others. In addition, a number of studies focused on specific geothermal systems have been published. Figure 2 resumes some exemplary electromagnetic studies carried out in the TVZ. Wairakei was the first geothermal system of the TVZ used for generation of electric power, and it was where the large resistivity contrast between hot geothermal waters and the background was first successfully demonstrated (for a detailed review on the electromagnetic studies at Wairakei see Bibby et al. 2009 and the references therein). Other well-studied geothermal systems include Rotokawa (e.g., Heise et al. 2008) and Ngatamariki (Risk et al. 2003). In all these geothermal fields, a

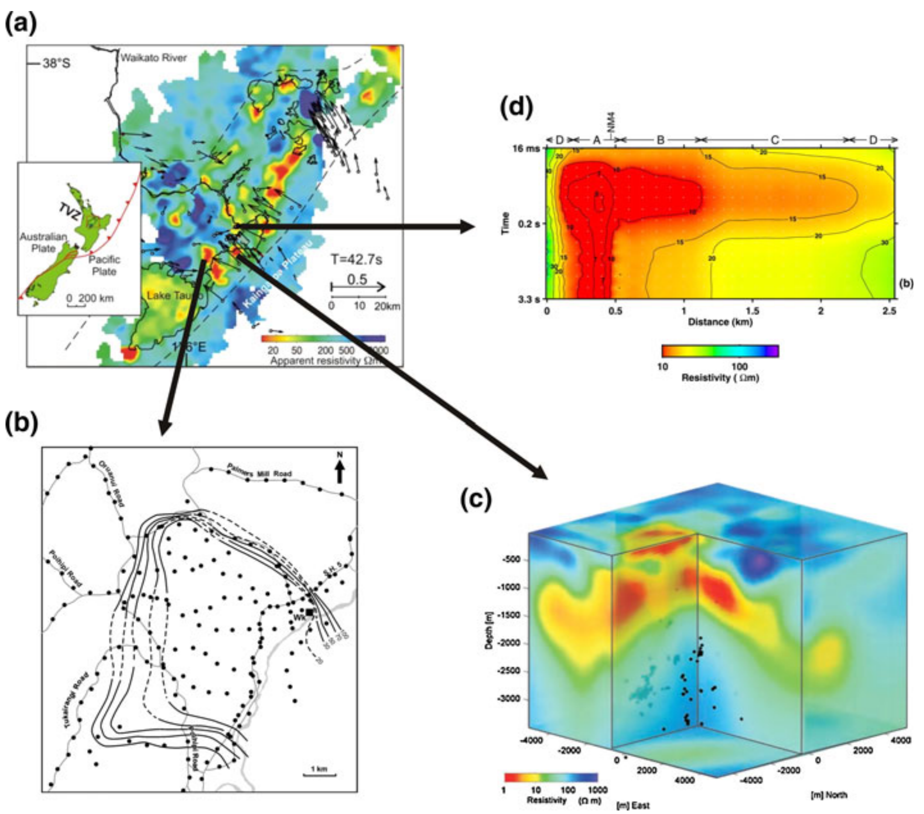

Fig. 2 Summary of some exemplary electromagnetic studies in the Taupo Volcanic Zone (TVZ) **a** DC apparent resistivity map of the TVZ obtained from Schlumberger array measurements using AB/2 = 500 m (after Bibby 1988). *Arrows* indicate location of the geothermal systems shown in the other panels. **b** *contour lines* of DC apparent resistivity obtained from Schlumberger array measurements in the Wairakei geothermal field (modified from Risk 1984). The low resistivity contour lines delineate the extent of the clay cap. **c** Three-dimensional electrical resistivity model obtained from 3D inversion of magnetotelluric (MT) data in the Rotokawa geothermal field. The low resistivity anomaly shows an elevated clay cap together with a higher resistivity core associated with temperatures >250 °C, the black dots represent seismic events located within the high resistivity core (after Heise et al. 2008). **d** Distance–time apparent resistivity pseudosection obtained from time-domain Eelectromagnetic (TDEM) measurements at the Ngatamariki geothermal field. A low resistivity feature associated with hydrothermal alteration is visible in the pseudosection (modified from Risk et al. 2003)

clear low resistivity anomaly associated with a clay cap has been delineated together with a deeper higher resistivity core associated with high-temperature alteration mineralogy.

3.2 Hengill Volcanic Zone (Iceland)

The Hengill volcanic complex is located at the southern end of the western volcanic zone of Iceland and is considered to be one of the largest high-temperature geothermal regions in the country. The Hengill complex hosts three volcanic centres whose products are mainly basalts and acidic rocks. Geothermal exploration in the Hengill area dates back to the 1940s, including a number of geophysical surveys (mostly documented in internal reports in Icelandic) such as DC resistivity (e.g., Hersir 1980), Bouguer gravity, central loop transient electromagnetic (TEM) or magnetotellurics (e.g., Hersir 1980; Oskooi et al. 2005; Árnason et al. 2010). The Hengill complex is of special relevance for electromagnetic exploration of geothermal resources because it was in the Nesjavellir geothermal field, just north of Mount Hengill, where the correlation between alteration mineralogy and electrical resistivity was first proposed (see Árnason et al. 2000 and references therein).

Árnason et al. (2010) presented a comprehensive electromagnetic study of the Hengill complex in which they obtained a three-dimensional resistivity distribution from joint 1D inversion of TEM and MT data and from 3D inversion of MT data. The dataset consists of 148 MT soundings acquired between 2000 and 2006 and more than 250 TEM soundings acquired since 1991. The TEM data, being unaffected by near-surface homogeneities of the electric field, can be used to correct the MT data for static shift effects, assuming the underlying structure is mostly one-dimensional in the first few metres and enough energy can be transmitted into the ground to ensure a good overlap between TEM and MT apparent resistivity curves. The authors performed a joint 1D inversion of TEM and MT (determinant) data and determined static shift factors which were subsequently used for correcting the MT data for separate 3D inversion.

The obtained 3D resistivity distribution shows a very coherent image between the stitched 1D joint inversions of TEM and MT and the 3D MT model. Figure 3 shows a cross-section of the resistivity distribution obtained from stitched 1D inversions along a 12-km-long profile crossing Mount Hengill. A low resistivity layer reflecting smectite-zeolite alteration is found at shallow depth (between 200 m a.s.l. and 800 m b.s.l.) being more elevated beneath Mount Hengill. At 800 m b.s.l., a high resistivity zone that was interpreted as an indication of high-temperature alteration extends to most of the survey area. A deeper low resistivity layer starts appearing beneath Mount Hengill at about 3,000 m b.s.l. At about 6,500 m b.s.l., it has extended to form a widespread conductor down to depths of about 10–15 km, where resistivity values reach 100 Ωm and higher. This deep conductive feature was interpreted as hot, solidified intrusions that act as heat sources for the geothermal system above (Árnason et al. 2010).

3.3 Western US

The west of the US, including areas such as the Basin and Range (B&R) physiographic province and Yellowstone, hosts a number of high-enthalpy geothermal systems, many of which are used for electricity generation. The B&R region is characterized by extensional tectonism that results in fault block mountains separated by alluvial valleys, high heat flow and seismicity and many active geothermal areas. In the B&R, geothermal systems are inherently open systems and are often accompanied by surface outflows. Although most of the presently known geothermal fields were discovered because of surface manifestations such as hot springs, fumaroles and hydrothermally altered ground, several electromagnetic methods have been successfully applied to detect and characterize the geothermal fields (see Fig. 4 for some exemplary electrical models from California).

Possibly, the most well known of the geothermal regions within the B&R is the Coso geothermal field in southern California. The basement of the Coso Range is dominated by fractured Mesozoic plutonic rocks that have been intruded by a large number of dikes, and partly covered by Late Cenozoic volcanics, consisting mainly of basalts and rhyolites. The emplacement history of the rhyolitic domes is consistent with either a single rhyolitic reservoir moving upward through the crust or a series of successively shallower reservoirs (Kurilovitch et al. 2003). This partially molten magma chamber is believed to be the heat

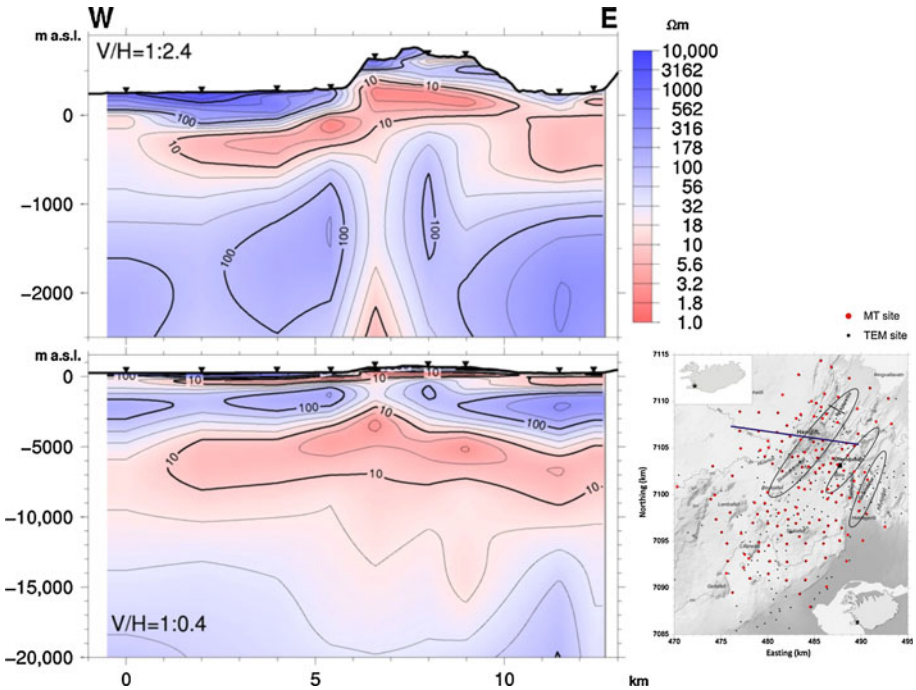

Fig. 3 Location map (*lower right panel*) of the MT (*red dots*) and TEM (*black dots*) stations in the survey area. Section location is indicated with a *blue line* in the map. Cross-sections (*left panels*) across the Hengill area obtained from stitched 1D joint inversion of TEM and determinant MT data. The *upper panel* focuses on the depth range down to 2,500 m b.s.l. and shows a shallow low resistivity layer reflecting smectite-zeolite alteration. The high resistivity below reflects high-temperature alteration. The *lower panel* shows the resistivity distribution down to depths of 20 km and highlights the presence of a deeper widespread low resistivity feature associated with hot, solidified intrusions that act as a heat source for the geothermal system above. Modified from Árnason et al. (2010)

source that drives the geothermal system (Wannamaker et al. 2004). Permeability is high within the individual Coso reservoirs but low in most of the surrounding rocks, limiting reservoir fluid recharge and making reinjection important for sustained productivity (Newman et al. 2008). A large number of electromagnetic surveys have been carried out in the Coso area (e.g., Wannamaker et al. 2004; Newman et al. 2005, 2008) revealing the classic MT response of a high-temperature geothermal reservoir, which presents a low resistivity hydrothermal alteration zone (smectite clay cap) located above and adjacent to more resistive propylitic alteration in the reservoir.

Similar low resistivity structures have also been observed in other areas of the western USA like the Glass Mountain geothermal resource area (Cumming and Mackie 2007, 2010) in northern California, the Beowave geothermal field (Garg et al. 2007) in Nevada, the Dixie Valley geothermal area also in Nevada (Garg et al. 2006; Wannamaker et al. 2007) or the Sulphur Springs thermal area in New Mexico (Wannamaker et al. 1997a, b).

3.4 Tuscany (Italy)

The geothermal systems in Tuscany (Italy) are concentrated in the Larderello—Travale area (Larsen et al. 1995; Fiordelisi et al. 1995; Manzella et al. 2006; 2010; Ooskoi and

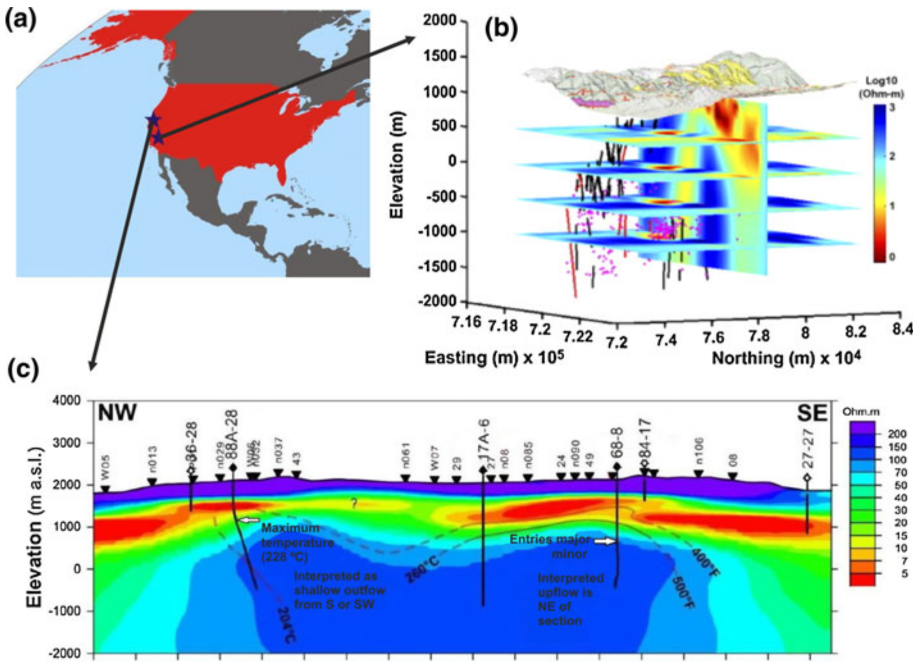

Fig. 4 **a** Location map of the Coso and Glass Mountain geothermal fields. **b** 3D electrical resistivity model of the Coso geothermal field obtained from 3D inversion of MT data (after Newman et al. 2008). **c** Cross-section of a 3D model obtained from inversion of the Zxy component of MT data corrected using TEM measurements in the Glass Mountain geothermal area (after Cumming and Mackie 2010). In both cases, the low resistivity anomaly associated with clay cap alteration mineralogy is clearly imaged over a higher resistivity high-temperature reservoir

Manzella 2011) and near the extinct volcano Mount Amiata (Fiordelisi et al. 2000; Volpi et al. 2003). These two systems represent interesting examples in the sense that although they are high-enthalpy geothermal systems, they do not conform to the classical electrical resistivity structure of a conductive clay cap overlying a high resistivity high-temperature reservoir core.

The Larderello—Travale (Fig. 5) system is a vapour dominated system with a deep reservoir defined by fractures within metamorphic rocks down to 4,000 m depth and characterized by very high temperatures up to 400 °C (Manzella et al. 2006). The Larderello—Travale area has been studied extensively using seismic methods (e.g., Brogi et al. 2003; Casini et al. 2010) whose main results comprise two reflective horizons (so-called H- and K-horizons) related to high productivity areas. The origin of the reflectivity of these horizons is considered to be related to the occurrence of localized high fluid pressure within fractured levels, although the underlying fracturing mechanism is still controversial (e.g., Marini and Manzella 2005). Resistivity models along 2D profiles in the Travale area (e.g., Manzella et al. 2006; Ooskoi and Manzella 2011) reveal high conductivity anomalies that the authors relate to a deep fractured and highly productive zone in the metamorphic rocks, thus being caused by high conductive geothermal fluids within a high permeability host.

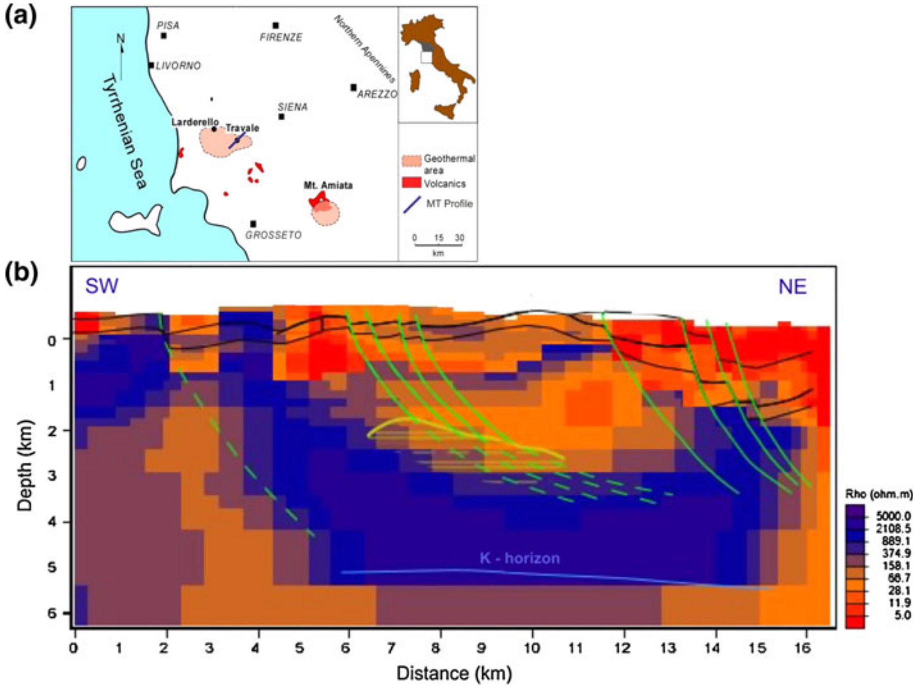

Fig. 5 **a** Location map of the Tuscany geothermal systems (Larderello, Travale, Mt. Amiata) and the Travale MT profile (*blue line*). Modified after Ooskoi and Manzella (2011). **b** Resistivity cross-section obtained from 2D inversion of MT data in the Travale geothermal area. High conductivity appears related to fractured high productivity zones in the metamorphic rocks (*green lines*). Modified after Manzella et al. (2006)

4 Non-Volcanic Geothermal Systems

Non-volcanic geothermal systems (including low-enthalpy systems, EGS, sedimentary reservoirs, etc.) are usually associated with hot fluids in sedimentary or crystalline reservoirs, either with natural permeability (through faults and fractures) or needing additional stimulation (EGS) of fluid pathways. In these systems, the aim of electromagnetic exploration is to image low resistivity anomalies correlated with saline geothermal fluids. Non-volcanic geothermal systems have been studied in a large variety of geographical and geological context such as in Bulgaria (Polyanovo, Bojadgieva et al. 2006), Philippines (Mabini, Del Rosario and Oanes 2010), Portugal (Chaves, Monteiro Santos et al. 1996, 2007), Korea (Pohang, Uchida et al. 2004, 2005; Lee et al. 2007), Brazil (Caldas Novas, Pastana de Lugao et al. 2002), France (Soultz-sous-Forêts, Geiermann and Schill 2010; Spichak et al. 2010) or Hungary (Szentlörinc, Yu et al. 2010; Tulinius et al. 2010). In the following section, I will highlight some examples of electromagnetic exploration of non-volcanic geothermal systems.

4.1 Llucmajor Aquifer System (Spain)

The Llucmajor aquifer system is located in the southern part of the island of Majorca (Spain). Water for agricultural purposes is extracted from the unconfined aquifer of the

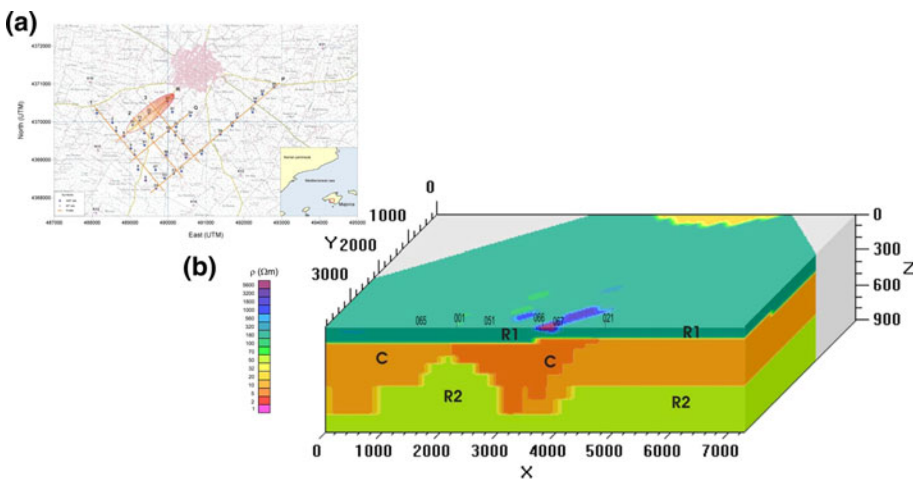

Fig. 6 **a** Location map of the Llucmajor aquifer system. The *black dots* represent the position of MT stations and the *red ellipse* the area with thermal manifestations. **b** Three-dimensional electrical resistivity distribution obtained from forward modelling by fitting the observed data through trial and error. The shallow and deep aquifers correspond with moderate/high resistivity regions, whereas the confining aquitard corresponds with low resistivity (Arango, pers. comm)

system. Some wells show a geothermal anomaly manifested by anomalous high water temperatures of 50 °C (Fig. 6). Because of the lack of heat sources in this region (volcanic or through heat generation in the rock matrix), these high values have been associated with vertical movements of water (Arango et al. 2009). An AMT–MT survey was carried out in 2002 to understand the aquifer system. A 3D resistivity model obtain from trial and error forward modelling of the AMT–MT data reveals a high resistive top layer, a more conductive middle layer, between 200 and 500 m, and a relatively resistive layer at the bottom. The main characteristic of the geoelectrical model is the thickness variation of the conductive layer, which presents minimum thickness in the area where the geothermal anomaly is located (Arango et al. 2009). The authors establish a simple conceptual model with two aquifers: one unconfined aquifer on top, and another deeper confined aquifer to supply the hot water, with the aquitard between both aquifers presenting a discontinuity (fault or fracture) to favour vertical fluid movements. An exploratory well drilled based on the results of the AMT data revealed a good coincidence of the resistivity model with the well logs and detected a layer of calcareous breccia which could be associated with the structure that allows warm water to rise (Arango et al. 2009). This very low-enthalpy resource represents an interesting example in the sense that the freshwater aquifers are imaged as moderate to high resistivity features, contrary to the more typical examples where the saline geothermal fluids have low resistivity signature.

4.2 Groß Schönebeck Geothermal Test Site (Germany)

The Groß Schönebeck in situ geothermal laboratory, located 40 km north of Berlin in northeastern Germany, is a key site for testing the geothermal potential of deep sedimentary basins. The target reservoir is located in Lower Permian sandstones and volcanic strata, which host deep aquifers throughout the Northeast German Basin (NEGB, Huenges et al. 2007). The laboratory consists of two 4.3-km-deep boreholes forming a geothermal

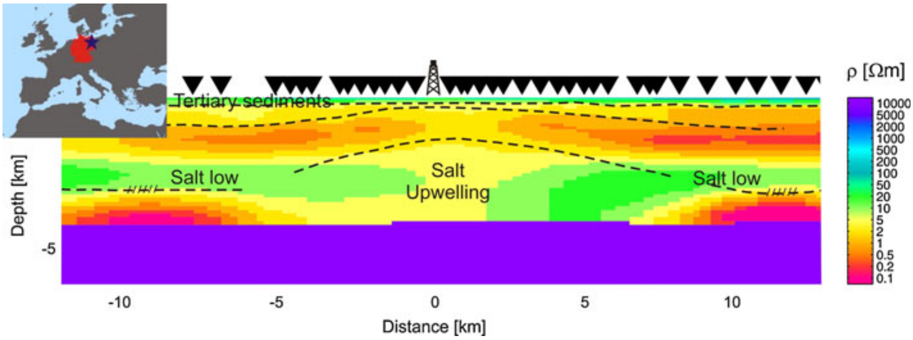

Fig. 7 Resistivity cross-section obtained from 2D inversion of MT data along a 40-km profile measured in the vicinity of the Groß Schönebeck geothermal test site (Germany). Shallow sediments were imaged as moderately resistive above a low resistivity layer with an antiform shape overlying a thick evaporitic sequence. Deep conductive anomalies associated with salt lows were interpreted as associated with highly fractured anhydrite rich areas enhancing hydraulic permeability (after the model from Muñoz et al. 2010a)

doublet system. The NEGB setting is typical for deep sedimentary basins and for low-enthalpy reservoirs in general. MT data were collected along two profiles to obtain a resistivity distribution of the Groß Schönebeck area (Muñoz et al. 2010a). Figure 7 shows the 2D resistivity model obtained from inversion of the MT data along the main profile. At surface, Tertiary sediments are imaged as a moderately conductive layer (20–50 Ωm), overlying a low resistivity layer which presents an antiform shape and coincides with the Mesozoic sedimentary sequences. At depth, two very low resistivity anomalies are obtained, coinciding with the reservoir level. These conductive bodies occur below the areas where the overlying evaporitic layer presents local lows, while only moderate resistivities are observed beneath the salt upwelling. In this context, the authors speculate that the reduced resistivity is associated with fracturing in brittle anhydrites, resulting in enhanced hydraulic permeability. This interpretation is supported by a statistical joint interpretation (Muñoz et al. 2010b) of the MT data together with coincident seismic tomography models (Bauer et al. 2010).

4.3 Puga Geothermal Area (India)

The Puga hot spring area, located to the south of the Indus Suture Zone in NW Himalaya, is considered to be the most promising geothermal field in India. The area exposes Pre-cambrian metamorphic rocks interlayered with bands of limestone and alluvium sediments on top and some younger granite intrusions of Tertiary age (Abdul Azeez and Harinarayana 2007). The high heat flow values obtained in thermal surveys have established the existence of a thermal anomaly in the Puga valley with over 100 hot springs with temperatures ranging from 35 to 84 °C and discharge rate up to 5 l/s (Shankar et al. 1976). An MT survey with 35 stations was carried out to explore the geothermal potential of the area (Harinarayana et al. 2004). Electrical resistivity cross-sections obtained from 2D inversion of the MT data (Fig. 8) show a near-surface low resistive (10–30 Ωm) zone of about 300–400 m thickness (A). The low resistive region, approximately 4 km in length, correlated well with the area marked by surface expressions of geothermal activity (Harinarayana et al. 2006). The authors explained the low resistivity of this layer by the varying thickness of alluvium sediments saturated with hot water or a mixture of deep thermal

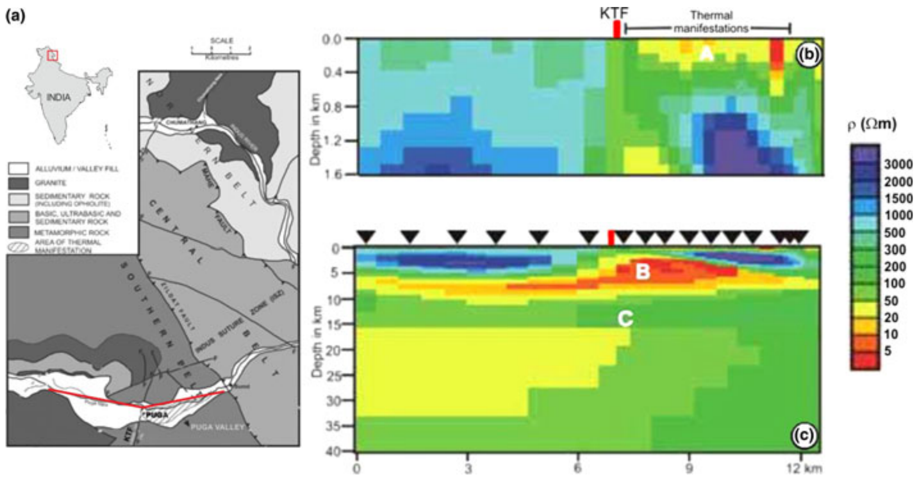

Fig. 8 **a** Location map of the Puga geothermal area and MT profile (*red line*). **b** Resistivity cross-section obtained from 2D inversion of the MT data for the first 1.6 km. A low resistivity area (*A*) appears east of the Kiagor Tatso fault, in the region where thermal manifestations are present. **c** Resistivity cross-section down to a depth of 40 km. Two low resistivity regions (*B* and *C*) are imaged at greater depths. Modified from Abdul Azeez and Harinarayana (2007)

water and freshwater, as observed in shallow wells, and considered it to be the shallow reservoir part of the geothermal field. No low resistivity structure was found west of the Kiagor Tatso fault, which marks the western boundary of the surface thermal manifestations. Another prominent feature imaged in the resistivity model was an anomalous low resistive structure (10–50 Ωm) from approximately 2–8 km depth below the geothermal manifestation and extending to the west (B). Underlying it, a 50 Ωm lower crust was found (C) (Abdul Azeez and Harinarayana 2007). The authors interpreted the low resistivity layer as a porous region with hot fluids located at the top of the magmatic heat source represented by the deeper moderate resistivity feature.

5 EGS Monitoring Tools

The importance of enhanced geothermal systems (EGS) for the development of geothermal energy is crucial (Tester et al. 2006). EM methods can provide important tools where advancements in subsurface characterization are imperative to develop EGS into a competitive industry. One significant complication in EGS development is estimating where injected fluids flow in the subsurface. EM methods, being sensitive to electrical resistivity contrast (between the low resistive injected fluids and the higher resistivity host rock), can be used as a supplementary tool to delineate reservoir boundaries. Few publications deal with application of EM methods for monitoring of temporal variations in subsurface electrical resistivity associated with geothermal fluid movement (e.g., Bedrosian et al. 2004; Aizawa et al. 2011) but interest is certainly increasing. Peacock et al. (2012a, b) present pioneering results from continuous MT measurements that show coherent changes generated from a fluid injection pilot experiment for an EGS at Paralana, South Australia. In July 2011, a volume of 3.1Ml of saline water (0.3 Ωm) was pumped into the intended reservoir at 3,680 m depth during 5 days. A star-shaped array of 30 MT stations (Fig. 9)

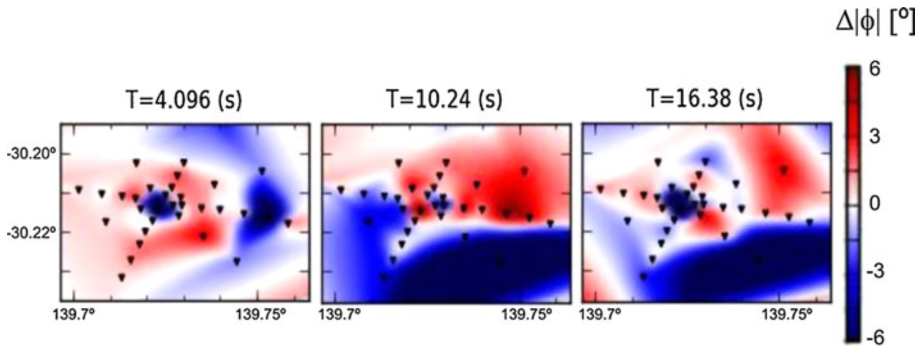

Fig. 9 Map view of phase tensor determinant residuals pre- and post-injection at different periods. *Black triangles* represent the location of MT stations. The borehole is centred within the cross of *black triangles*. *Red colours* indicate a conductive change and blue a resistive change. The conductive anomaly NE of the borehole was interpreted as caused by fluid migration in a NE preferred direction (modified from Peacock et al. 2012b)

was deployed before injection to measure a base line, and measurements were repeated after the injection had been completed. The variations in MT parameters (apparent resistivity, impedance phase and phase tensor parameters) were estimated by computing residuals of pre- and post-injection values (Peacock et al. 2012a). Figure 9 shows phase tensor determinant residuals of before and after fluids are introduced into the system for all sites and various periods. Red colours indicate a change towards higher conductivities and blue colours a change towards lower conductivities. A conductive anomaly located to the right of the borehole observed at periods from 2 to 16 s was interpreted as a complex reservoir evolution to the NE of the borehole, expanding in a NE preferred orientation (Peacock et al. 2012a).

6 Misinterpretation of Electrical Resistivity Data in Geothermal Systems

Electromagnetic methods have proven to be very successful for delineating geothermal systems, as reported in the previous sections, and have become industry standard for exploration of geothermal resources. This success, however, has resulted sometimes in careless and inaccurate interpretation based on the belief that electrical resistivity data can be interpreted correlating one-to-one areas of low resistivity with presence of geothermal fluids and/or conducting clay minerals produced by hydrothermal alteration. This exploration approach, which some authors call “anomaly hunting”, can lead to severe misinterpretations of electrical resistivity data.

While many known geothermal systems have a low resistivity signature, the converse is not true; the existence of low resistivity zones in a geothermal area does not necessarily imply an active hydrothermal systems. An alteration which produces the low resistivity of the clay cap is unaffected by subsequent cooling, that is, even if the temperatures that produced the alteration mineralogy do not prevail the clay cap still presents a low resistivity signature. For instance, to the SE of the Hengill geothermal field in Iceland, the resistivity structure derived from a TEM sounding revealed alteration mineralogy consistent with drilled cores (Árnason and Magnússon 2001). A resistive core, which would be indicative of temperatures above 240 °C within a hot geothermal system, was found as shallow as at 200 m depth, whereas the temperatures in the well were measured under 200 °C to a depth of 1,000 m. At the Krafla geothermal field, also in Iceland, Árnason et al. (2000) report resistivity structures in agreement with alteration. However, a well drilled in an area where the resistivity pattern was interpreted as indicating high temperature measured surprisingly cold temperatures below 100 °C between 700 and 1,400 m depth (Mortensen 2009).

Moreover, the causes of low resistivity structures could be unrelated to a geothermal system, even in an active geothermal area. Bibby et al. (2005) report on an exploratory well drilled down to a depth of 593 m in the Matahana basin near the Horohoro geothermal field in the TVZ of New Zealand in 1986. The well targeted the northern limit of a deep low resistivity zone revealed by a DC Schlumberger array using AB/2 = 1,000 m. It was postulated that this low resistivity zone represented a deep geothermal system from which thermal fluids flowed laterally to reach the surface at the nearby Horohoro springs. Temperatures at hole bottom reached a maximum of 80 °C, and no geothermal fluids were found in the hole, indicating a non-geothermal origin of the low resistivity anomaly. Subsequent regional resistivity mapping (Bibby 1988) indicated that this deeper low resistivity anomaly could be part of a conductive layer with regional extent. Bibby et al. (2005) interpreted this regional low resistivity layer as associated with old ignimbrites (>1 Ma). Petrological studies of these ignimbrites show that they contain low-temperature hydrothermal alteration products (Allis 1987) which allow electric conduction along crystalline interfaces and result in its characteristic low resistivity values.

Another example of a misinterpretation of a low resistivity anomaly in the context of a geothermal resource exploration in the Menderes massif can be found in Kuyumcu et al. (2011). The Menderes massif is a major metamorphic complex in western Turkey with geothermal potential. A three-dimensional resistivity model obtained from an extended MT survey in the Tire area, over the central Menderes massif, reveals a widespread intra-basement conductor dipping down to the north and to the west (Fig. 10). A striking low resistivity anomaly like this might look appealing as a hot fluid geothermal target. A first exploration well (Tire-1) was drilled down to a depth of 2,325 m, resulting in a temperature of only 85 °C and a flow rate of 4 l/min. Rock samples collected from the well at various depths were analyzed with X-ray diffraction revealing pelitic schist and gneiss formations with significant graphite content. In this context, graphite was interpreted as the most likely cause of the low resistivity in the basement. Kuyumcu et al. (2011) point out that the region was already known to have shear zones, some with graphitic units, prior to drilling the exploration well.

Three-dimensional MT inversion of a dataset collected in the Krafla volcanic complex in northeastern Iceland (Gasperikova et al. 2011) revealed a highly resistive layer near the surface, which was identified as unaltered basalt, covering a low resistivity cap corresponding to the smectite-zeolite zone. Below this area, an increase in resistivity could correspond to the chlorite-epidote zone. Although this resistivity distribution, correlated with alteration mineralogy rather than lithology, pointed to a classical hydrothermal system, and the high resistivity core seemed to be a suitable target for drilling, the Iceland Deep Drilling Programme (IDDP) well at Krafla encountered magma at the depth of 2.1 km and drilling was stopped (Gasperikova et al. 2011). This does not represent a misinterpretation of resistivity data in the same sense as the previous examples, but rather illustrates the fact that MT is sensitive to large geological structures but not to individual fractures, in this case filled with magma. Other studies in the same area (Einarsson 1978; Mortensen et al. 2010) suggested possible shallow magma chambers in the region.

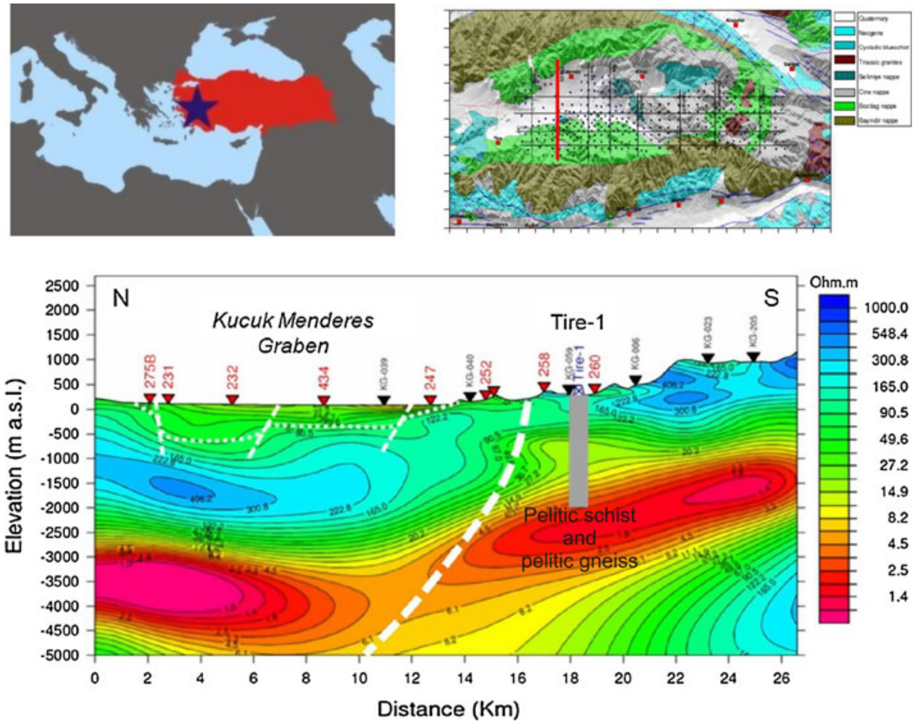

Fig. 10 Resistivity cross-section along a profile (*upper panel*) obtained from 2D inversion of MT data in the Menderes massif (western Turkey). Although the resistivity model clearly images a low resistivity anomaly at 2–4 km depth, which could represent a very attractive geothermal drill target, the 2,500 m deep Tire-1 well encountered politic schist and gneiss and the area was deemed unsuitable for geothermal exploitation (modified from Kuyumcu et al. 2011)

To minimize misinterpretations of electrical resistivity models, it is necessary to avoid "anomaly hunting" and proceed carefully with integration of as much data as possible into conceptual models of the geothermal systems. Figure 11 shows a hypothetical exploration scenario in a prospect with sediments overlying fractured metamorphic rocks (based on Cumming 2009) and illustrates the possible process of building a conceptual model and designing further exploration activities. Panel a) shows the electrical resistivity distribution (obtained from, e.g., MT inversion) together with some known geological information (surface trace of an imaged fault and surface lithologies). The only surface manifestation is a (now inactive) travertine deposit. A sensible starting assumption would be to interpret the particular low resistivities of the sediments as clay rich and impermeable. The deep low resistivity anomaly located left of the fault, being located in Palaeozoic metamorphic schists, has the potential to be related to graphitic conduction and therefore should be ignored in the first stage of geothermal exploration. Since there are no surface manifestations associated with the fault trace, if a viable reservoir is present, it is reasonable that the possible upflow occurs along secondary fractures right of the fault, beneath the area where the clay cap (<5 Ωm) reaches its maximum depth (see, e.g., the Conceptual model section in this paper or Pellerin et al. 1996). The geometry of the flat resistive area covered by shallow conductive sediments suggests a possible outflow related to the deposition of travertines (see, e.g., the Conceptual model section in this paper or Anderson et al. 2000), whose presence implies

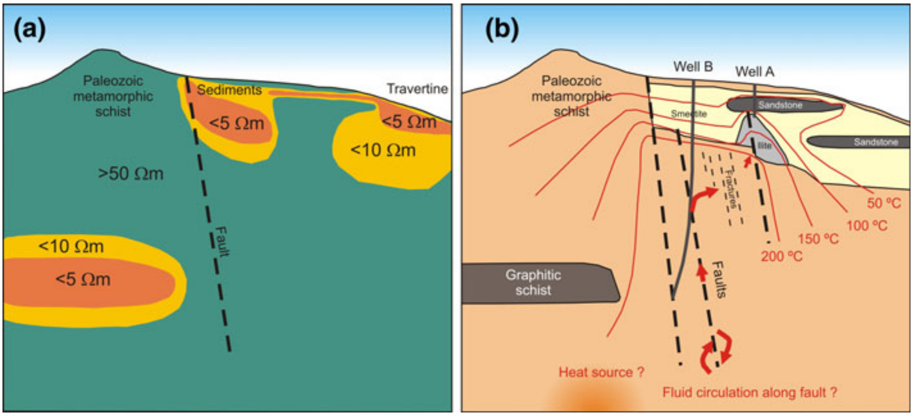

Fig. 11 **a** Results of a hypothetical electrical resistivity survey and some known geological features. **b** Possible conceptual model of the geothermal system. See text for details on the development of the conceptual model (redrawn after Cumming 2009)

exposure to a temperature of about 180 °C at some previous time. The inactivity of the travertine deposit might be attributed to a drop in the water table (see, e.g., Cumming 2009). Possible further exploration step could be a shallow (250 m) exploration well (well A in Fig. 11b) to obtain water samples from the high resistivity outflow zone (aquifer) and a shallow seismic survey to localize fractured regions. To continue this hypothetical scenario, let us assume that the exploration well reveals silicified sandstones with a temperature of 100 °C at 250 m depth, with cation geothermometry of 200 °C at the well bottom and the seismic image reveals several fractures nearby the mapped fault. Based on this data, a second deeper well (well B in Fig. 11b) could be planned to be drilled directionally across as many structures as possible in order to establish a complete conceptual model and as a potential exploitation well. For more details on this exploration scenario see Cumming (2009).

7 Conclusions

EM exploration of geothermal zones provides a useful contribution to geothermal exploration and exploitation. Given the nature of the geothermal reservoirs, both high-enthalpy hydrothermal systems and non-volcanic systems, electrical resistivity is a key parameter (perhaps the key parameter) for exploration and the development of conceptual models. In hydrothermal systems, electrical resistivity is dominated by alteration mineralogy, which can be used as a useful proxy for temperature and therefore constrain the properties of geothermal systems. In non-volcanic reservoirs, saline geothermal fluids and their flow paths (faults and fractures) can be imaged by EM methods. Knowing the conductivity of the fluids, it is possible to establish sensible estimates of porosity and/or permeability of the system, which are important reservoir parameters. EM exploration of geothermal systems is mostly a story of success, but the relationship between low resistivity anomalies and geothermal targets should not be carried too far (avoid anomaly hunting) to not avoid interpretation pitfalls which can result in expensive drilling exercises. Development of conceptual models, based on electrical resistivity data, but incorporating geological, geochemical, temperature and/or other geophysical data becomes a necessity when it comes to the ultimate goal of exploration: understand the system.

Acknowledgments I would like to thank the Program Committee of the 21st Electromagnetic Induction Workshop for giving me the opportunity to write this review paper. My attendance to the workshop was financed by the project Brine (Grant Nr. 03G0758A/B) funded by the German Federal Ministry of Education and Research. I also thank all authors who sent me their papers, manuscripts and conference contributions, which helped me a lot in writing this review paper, and I apologise for any omissions. This paper has been improved by the comments of my colleague Ute Weckmann, Knútur Árnason and an anonymous reviewer.

References

Abdul Azeez KK, Harinarayana T (2007) Magnetotelluric evidence of potential geothermal resource in Puga, Ladakh, NW Himalaya. Curr Sci 93:323–329

Abiye TA, Haile T (2008) Geophysical exploration of the Boku geothermal area, Central Ethiopian Rift. Geothermics 37:586–596

Aizawa K, Kanda W, Ogawa Y, Iguchi M, Yokoo A, Yakiwara H, Sugano T (2011) Temporal changes in electrical resistivity at Sakurajima Volcano from continuous magnetotelluric observations. J Volcanol Geoth Res 199:165–175

Allis RG (1987) Geophysics and geochemical investigations of the Horohoro geothermal prospect. Report. 213, Geophysics Division, DSIR, Wellington, pp 78

Anderson E, Crosby D, Ussher G (2000) Bulls-eye! Simple resistivity imaging to reliably locate the geothermal reservoir. In: proceedings world geothermal congress, Kyushu-Tohoku, Japan, pp 909–914

Arango C, Marcuello A, Ledo J, Queralt P (2009) 3D magnetotelluric characterization of the geothermal anomaly in the Llucmajor aquifer system (Majorca, Spain). J Appl Geophys 68:479–488

Árnason K, Flovenz ÓG (1998) Geothermal exploration by TEM-soundings in the Central Asal Rift in Djibouti, East Africa. In: proceedings world geothermal congress, Florence, Italy, pp 933–938

Árnason K, Magnússon IÞ (2001) Geothermal Activity in Hengill and Hellisheiði. Results of Resistivity Surveys. Orkustofnun Report OS-2001/091, Reykjavik, Iceland, pp 250 (in Icelandic)

Árnason K, Karlsdóttir R, Eysteinsson H, Flóvenz ÓG, Guðlaugsson STh (2000) The resistivity structure of high-temperature geothermal systems in Iceland. In: proceedings world geothermal congress, Tohoku-Kyushu, Japan, pp 923–928

Árnason K, Eysteinsson H, Hersir GP (2010) Joint 1D inversion of TEM and MT data and 3D inversion of MT data in the Hengill area, SW Iceland. Geothermics 39:13–34

Asaue H, Koike K, Yoshinaga T, Takakura S (2005) Magnetotelluric resistivity modeling for 3D characterization of geothermal reservoirs in the Western side of Mt. Aso, SW Japan. J Appl Geophys 58:296–312

Barbier E (2002) Geothermal energy technology and current status: an overview. Renew Sustain Energy Rev 6:3–65

Bauer K, Moeck I, Norden B, Schulze A, Weber M, Wirth A (2010) Tomographic P-wave velocity and vertical velocity gradient structure across the geothermal site Groß Schönebeck (NE German Basin): relationship to lithology, salt tectonics, and thermal regime. Journal of geophysical Research 115, doi: 10.1029/2009JB006895

Bedrosian PA, Weckmann U, Ritter O, Hammer CU, Hübert J, Jung A (2004) Electromagnetic monitoring of the Groß Schönebeck stimulation experiment. In: proceedings Jahrestagung der Deutschen Geophysikalischen Gessellschaft, p 64, GFZ, Berlin

Benderitter Y, Cormy G (1990) Possible approach to geothermal research and relative costs. In: Dickson MH, Fanelli M (eds) Small geothermal resources: a guide to development and utilization. UNITAR, New York, pp 59–69

Bertani R (2010) Geothermal power generation in the world. 2005–2010 Update Report. In: proceedings world geothermal congress, Bali, Indonesia

Bertrand EA, Caldwell TG, Hill GJ, Wallin EL, Bennie SL, Cozens N, Onacha SA, Ryan GA, Walter C, Zaino A, Wameyo P (2012) Magnetotelluric imaging of upper-crustal convection plumes beneath the Taupo Volcanic Zone, New Zealand. Geophys Res Lett 39:L02304. doi:10.1029/2011GL050177

Bibby HM (1988) Electrical resistivity mapping in the Central Volcanic Region of New Zealand. NZ J Geol Geophys 31:259–274

Bibby HM, Caldwell TG, Davey FJ, Webb TH (1995) Geophysical evidence on the structure of the Taupo Volcanic Zone and its hydrothermal circulation. J Volcanol Geoth Res 68:29–58

Bibby HM, Caldwell TG, Risk GF (2002) Long offset tensor resistivity surveys of the Taupo Volcanic Zone, New Zealand. J Appl Geophys 49:17–32

Bibby HM, Risk GF, Caldwell TG, Bennie SL (2005) Misinterpretation of electrical resistivity data in geothermal prospecting: a case study from the Taupo Volcanic Zone. In: proceedings world geothermal congress, Antalya, Turkey

Bibby HM, Risk GF, Caldwell TG, Heise W (2009) Investigations of deep resistivity structures at the-Wairakei geothermal field. Geothermics 38:98–107

Björnsson A, Hersir GP, Björnsson G (1986) The Hengill high-temperature area, S.W. Iceland: regional Geophysical Survey. Trans Geotherm Res Counc 10:205–210

Brogi A, Lazzarotto A, Liotta D, Ranalli G (2003) Extensional shear zones as imaged by reflection seismic lines: the Larderello geothermal field (central Italy). Tectonophysics 363:127–139

Bojadgieva K, Hristov V, Srebrov B, Harinarayana T, Veeraswamy K (2006) Temperature investigation in Polyanovo hydrothermal reservoir (SE Bulgaria). Bulg Geophys J 32:3–11

Burçak M, Kaya C, Riza Kılıç A, Akdogan N (2005) Exploration of the heat source and geothermal possibilities of the Aksaray Region, Central Anatolia, Turkey. In: proceedings world geothemal congress, Antalya, Turkey

Caldwell G, Pearson C, Zayadi H (1986) Resistivity of rocks in geothermal systems: a laboratory study. In: proceedings 8th NZ geothermal workshop, pp 227–231

Casini M, Ciuffi M, Fiordelisi A, Mazzotti A, Stucchi E (2010) Results of a 3D seismic survey at the Travale (Italy) test site. Geothermics 39:4–12

Cumming W (2009) Geothermal resource conceptual models using surface exploration data. In: proceedings, 34th workshop on geothermal reservoir engineering, Stanford University

Cumming W, Mackie R (2007) 3D MT resistivity imaging for geothermal resource assessment and environmental mitigation at the glass mountain KGRA, California. GRC Transactions 31:331–334

Cumming W, Mackie R (2010) Resistivity imaging of geothermal resources using 1D, 2D and 3D MT inversion and TDEM static shift correction illustrated by a glass mountain case history. In: proceedings world geothemal congress, Bali, Indonesia

Daud Y, Sudarman S, Ushijima K (2001) Imaging reservoir permeability of the Sibayak geothermal field, Indonesia using geophysical measurements. In: proceedings, 26th workshop on geothermal reservoir Engineering, Stanford University

Deer WA, Howie RA, Zussman J (1962) Rock-forming minerals, Vol 3 sheet silicates. Longmans, Green and Co Ltd, London, p 270

Del Rosario R, Oanes AF (2010) Controlled source magnetotelluric survey of Mabini geothermal prospect, Mabini, Batangas, Philippines. In: proceedings world geothemal congress, Bali, Indonesia

Einarsson P (1978) S-wave shadows in the Krafla caldera in NE-Iceland, evidence for a magma chamber in the crust. Bull Volcanol 41:187–195

Essene EJ, Peacor DR (1995) Clay mineral thermometry; a critical perspective. Clays Clay Miner 43:540–553

Fiordelisi A, Mackie RL, Madden T, Manzella A, Rieven SA (1995) Application of the magnetotelluric method using a remote—remote reference system for characterizing deep geothermal system. In: proceedings world geothemal congress, Florence, Italy, pp 893–897

Fiordelisi A, Manzella A, Buonasorte G, Larsen JC, Mackie RL (2000) MT methodology in the detection of deep, water-dominated geothermal systems. In: proceedings world geothemal congress, Tohoku-Kyushu, Japan, pp 1121–1126

Garg SK, Pritchett JW, Combs J (2006) Characterization of geothermal reservoir conditions using electrical surveys: some preliminary results. GRC Transactions 30:419–424

Garg SK, Pritchett JW, Wannamaker PE, Combs J (2007) Characterization of geothermal reservoirs with electrical surveys: beowawe geothermal field. Geothermics 36:487–517

Gasperikova E, Newman G, Feucht D, Arnason K (2011) 3D MT characterization of two geothermal fields in Iceland. GRC Transactions 35:1667–1671

Geiermann J, Schill E (2010) 2-D magnetotellurics at the geothermal site at Soultz-Sous-Forets- resistivity distribution to about 3000 M Depth. Comptes Rendus Geoscience. doi:10.1016/j.crte.2010.04.001

Harinarayana T, Abdul Azeez KK, Naganjaneyulu K, Manoj C, Veeraswamy K, Murthy DN, Prabhakar Eknath Rao S (2004) Magnetotelluric studies in Puga valley geothermal field, NW Himalaya, Jammu and Kashmir, India. J Volcanol Geoth Res 138:405–424

Harinarayana T, Abdul Azeez KK, Murthy DN, Veeraswamy K, Eknath Rao SP, Manoj C, Naganjaneyulu K (2006) Exploration of geothermal structure in Puga geothermal field, Ladakh Himalayas, India by magnetotelluric studies. J Appl Geophys 58:280–295

Heise W, Bibby HM, Caldwell TG, Bannister SC, Ogawa Y, Takakura S, Uchida T (2007) Melt distribution beneath a young continental rift: the Taupo volcanic zone, New Zealand. Geophys Res Lett 34:L14313. doi:10.1029/2007GL029629

Heise W, Caldwell TG, Bibby HM, Bannister SC (2008) Three-dimensional modelling of magnetotelluric data from the Rotokawa geothermal field, Taupo Volcanic Zone, New Zealand. Geophys J Int 173:740–750. doi:10.1111/j.1365-246X.2008.03737.x

Hersir GP (1980) Electric and electromagnetic measurements across the Mid-Atlantic Ridge in Southwest Iceland, with special reference to the high temperature area of Hengill. M. Sc. Thesis. University of Aarhus, Denmark, pp 165

Huenges E, Moeck I, the geothermal group of the GFZ (2007) Directional drilling and stimulation of a deep sedimentary geothermal reservoir. Sci Drill 5:47–49

Kurilovitch L, Norman D, Heizler M, Moore J, McCulloch J (2003) 40Ar/39Ar Thermal History of the Coso Geothermal Field. In: proceedings, 28th workshop on geothermal reservoir engineering, Stanford University

Kuyumcu ÖC, Destegül Solaroglu UZ, Hallinan S, Çolpan B, Turkoglu E, Soyer W (2011) Interpretation of 3D Magnetotelluric (MT) Surveys: basement conductors of the Menderes Massif, Western Turkey. GRC Transactions 35:861–866

Lagios E, Galanopoulos D, Hobbs BA, Dawes GJK (1998) Two-dimensional magnetotelluric modelling of the Kos Island geothermal region (Greece). Tectonophysics 287:157–172

Larsen J, Mackie R, Fiordelisi A, Manzella A, Rieven S (1995) Robust processing for removing train signals from Magnetotelluric Data in Central Italy. In: proceedings world geothemal congress, Florence, Italy, pp 903–908

Lee TJ, Song Y, Uchida T (2007) Three-dimensional magnetotelluric surveys for geothermal development in Pohang, Korea. Explor Geophys 38:44–49

Manzella A, Spichak V, Pushkarev P, Sileva D, Oskooi B, Ruggieri G, Sizov Y (2006) Deep fluid circulation in the travale geothermal area and its Relation with Tectonic Structure Investigated by a Magnetotelluric Survey. In: proceedings, 31st workshop on geothermal reservoir engineering, Stanford University

Manzella A, Ungarelli C, Ruggieri G, Giolito C, Fiordelisi A (2010) Electrical resistivity at the Travale geothermal field (Italy). In: proceedings world geothemal congress, Bali, Indonesia

Marini L, Manzella A (2005) Possible seismic signature of the α–β quartz transition in the lithosphere of Southern Tuscany (Italy). J Volcanol Geoth Res 148:81–97

Meju MA (2002) Geoelectromagnetic exploration for natural resources: models, case studies and challenges. Surv Geophys 23:133–205

Monteiro Santos FA, Dupis A, Andrade Afonso AR, Mendes-Victor LA (1996) An audiomagnetotelluric survey over the Chaves geoth geothermal field (NE Portugal). Geothermics 25:389–406

Monteiro Santos FA, Andrade Afonso AR, Dupis A (2007) 2D joint inversion of DC and scalar audiomagnetotelluric data in the evaluation of low enthalpy geothermal fields. J Geophys Eng 4:53–62

Mortensen AK (ed), Guðmundsson Á, Sigmundsson F, Axelsson G, Ármannsson H, Björnsson H, Ágústsson K, Sæmundsson K, Ólafsson M, Karlsdóttir R, Halldórsdóttir S, Hauksson T (2009) Krafla Geothermal System. A compilation of explorations and developments of the geothermal system and a reevaluation of the conceptual model. Landsvirkjun Report LV-2009/111 and ÍSOR, ÍSOR-2009/057, Reykjavik, Iceland, pp 180 (in Icelandic)

Mortensen AK, Grönvold K, Guðmundsson A, Steingrímsson B, Egilson T (2010) Quenched silicic glass from well K-39 in Krafla, North-Eastern Iceland. In: proceedings world geothermal congress, Bali, Indonesia

Muffler P, Cataldi R (1978) Methods for regional assessment of geothermal resources. Geothermics 7:53–89

Mulyadi (2000) Magnetotelluric method applied for geothermal exploration in Sibayak, North Sumatra. In: proceedings world geothemal congress, Tohoku-Kyushu, Japan, pp 1469–1472

Muñoz G, Ritter O, Moeck I (2010a) A target-oriented magnetotelluric inversion approach for characterizing the low enthalpy Groß Schönebeck geothermal reservoir. Geophys J Int 183:1199–1215

Muñoz G, Bauer K, Moeck I, Schulze A, Ritter O (2010b) Exploring the Groß Schönebeck (Germany) geothermal site using a statistical joint interpretation of magnetotelluric and seismic tomography models. Geothermics 39:35–45

Muraoka H, Uchida T, Sasada M, Yagi M, Akaku K, Sasaki M, Yasukawa K, Miyazaki S, Doi M, Saito S, Sato S, Tanakam S (1998) Deep geothermal resources survey program: igneous, metamorphic and hydrothermal processes in a well encountering 500 °C at 3729 m Depth, Kakkonda, Japan. Geothermics 27:507–534

Mwangi AW (2012) Eburru Geothermal Prospect, Kenya —Joint 1D Inversion of MT and TEM Data. In: proceedings, 37th workshop on geothermal reservoir Engineering, Stanford University

Newman GA, Hoversten M, Gasperikova E, Wannamaker PE (2005) 3D magnetotelluric characterization of the Coso geothermal field. In: proceedings, 30th workshop on geothermal reservoir Engineering, Stanford University

Newman GA, Gasperikova E, Hoversten GM, Wannamaker PE (2008) Three-dimensional magnetotelluric characterization of the Coso geothermal field. Geothermics 37:369–399
Nurmukhamedov AG, Chernev II, Alekseev DA, Yakovlev AG (2010) 3D geoelectric model of the Mutnov steam hydrothermal deposit. Phys Solid Earth 46:739–750
Ogawa Y, Bibby HM, Caldwell TG, Takakura S, Uchida T, Matsushima N, Bennie SL, Tosha T, Nishi Y (1999) Magnetotelluric image of the Taupo Volcanic Zone, New Zealand. Geophys Res Lett 26:3673–3676
Ooskoi B, Manzella A (2011) 2D inversion of the Magnetotelluric data from Travale geothermal field in Italy. J Earth Space Phys 36:1–18
Oskooi B, Pedersen LB, Smirnov M, Árnason K, Eysteinsson H, Manzella A, the DGP Working Group (2005) The deep geothermal structure of the Mid-Atlantic Ridge deduced from MT data in SW Iceland. Phys Earth Planet Inter 150:183–195
Pastana de Lugao P, LaTerra EF, Kriegshäuser B, Fontes SL (2002) Magnetotelluric studies of the Caldas Novas geothermal reservoir, Brazil. J Appl Geophys 49:33–46
Peacock JR, Thiel S, Reid P, Heinson G (2012a) Magnetotelluric monitoring of a fluid injection: Example from an enhanced geothermal system. Geophysical Research Letters 39, doi:10.1029/2012GL053080
Peacock JR, Thiel S, Reid P, Messellier M, Heinson G (2012b) Monitoring enhanced geothermal fluids with magnetotellurics, test case: Paralana, South Australia. In: proceedings, 37th workshop on geothermal reservoir Engineering, Stanford University
Pellerin L, Johnston JM, Hohmann GW (1996) A numerical evaluation of electromagnetic methods in geothermal exploration. Geophysics 61:121–130
Raharjo IB, Maris V, Wannamaker PE, Chapman DS (2010) Resistivity Structures of Lahendong and Kamojang geothermal systems revealed from 3-D Magnetotelluric Inversions, a Comparative Study. In: proceedings world geothemal congress, Bali, Indonesia
Risk GF, Caldwell TG, Bibby HM (2003) Tensor time-domain electromagnetic resistivity measurements at Ngatamariki geothermal field, New Zealand. J Volcanol Geoth Res 127:33–54
Ritter O, Hoffmann-Rothe A, Bedrosian PA, Weckmann U, Haak V (2005) Electrical conductivity images of active and fossil fault zones. In: Bruhn D and Burlini L (eds), High Strain Zones: Structure and Physical Properties, The Geological Society, pp 165–186
Romo JM, Flores C, Vega R, Vázquez R, Pérez Flores MA, Gómez Treviño E, Esparza FJ, Quijano JE, García VH (1997) A closely-spaced magnetotelluric study of the Ahuachapán-Chipilapa geothermal field, El Salvador. Geothermics 26:627–656
Rybach L (2010) Status and prospects of geothermal energy. In: proceedings world geothermal congress, Bali, Indonesia
Shankar R, Padhi RN, Prakash G, Thussu JL, Wangdus C (1976) Recent geological studies in upper Indus valley and the plate tectonics. Geol Surv India, Misc Publ 34:41–56
Spichak V (2005) Three-dimensional resistivity structure of the Minamikayabe geothermal zone revealed by Bayesian inversion of MT Data. In: proceedings world geothemal congress, Antalya, Turkey
Spichak V, Manzella A (2009) Electromagnetic sounding of geothermal zones. J Appl Geophys 68:459–478
Spichak V, Schwartz Y, Nurmukhamedov AG (2007) Conceptual Model of the Mutnovsky Geothermal Deposit (Kamchatka) Based on electromagnetic, gravity and magnetic data. In: Proceedings, EGM international workshop
Spichak V, Geiermann J, Zakharova O, Calcagno P, Genter A, Schill E (2010) Deep temperature extrapolation in the Soultz-sous-Forêts geothermal area using magnetotelluric data
Stagpoole VM, Bibby HM (1998) The shallow resistivity structure of the Taupo Volcanic Zone, New Zealand. In: Proceedings of the 20th N.Z. geothermal workshop, University of Auckland Geothermal Institute, pp 303–310
Tester JW and the MIT geothermal panel (2006) The future of geothermal energy—impact of enhanced geothermal systems (EGS) on the United States in the 21st Century, MIT—Massachusetts Institute of Technology, Cambridge, MA. p 358
Tulinius H, Þorbergsdóttir IM, Ádám L, Hu ZZ, Yu G (2010) Geothermal evaluation in Hungary using integrated interpretation of well, seismic, and MT data. In: proceedings world geothemal congress, Bali, Indonesia
Uchida T (1995) Resistivity structure of Sumikawa geothermal field, northeastern Japan, obtained from magnetotelluric data. In: proceedings world geothemal congress, Florence, Italy, pp 921–925
Uchida T (2005) Three-dimensional magnetotelluric investigation in geothermal fields in Japan and Indonesia. In: proceedings world geothemal congress, Antalya, Turkey
Uchida T, Ogawa Y, Takakura S, Mitsuhata Y (2000) Geoelectrical investigation of the kakkonda geothermal field, Northern Japan. In: proceedings world geothemal congress, Tohoku-Kyushu, Japan, pp 1893–1898

Uchida T, Lee TJ, Honda M, Andan A (2002) 2-D and 3-D interpretation of magnetotelluric data in the Bajawa geothermal field, central Flores, Indonesia. Bull Geol Surv Japan 53:265–283
Uchida T, Song T, Lee TJ, Mitsuhata Y, Lee SK, Lim SK (2004) 3D magnetotelluric interpretation in Pohang low-enthalpy geothermal area, Korea. In: proceedings 17th electromagnetic induction workshop, Hyderabad, India
Uchida T, Song Y, Lee TJ, Mitsuhata Y, Lee SK, Lim SK (2005) Magnetotelluric survey in an extremely noisy environment at the pohang low-enthalpy geothermal area, Korea. In: proceedings world geothermal congress, Antalya, Turkey
Uchida T, Takakura S, Ueda T, Adachi M, Ozeki M, Kamada K, Sato T (2010) 3D magnetotelluric survey at the Yanaizu-Nishiyama geothermal field, Northern Japan. In: Proceedings of the 9th Asian Geothermal Symposium, pp 26–31
Ucok H, Ershaghi I, Olhoeft G (1980) Electrical resistivity of geothermal brines. J Petrol Technol 32:717–727
Ussher G, Harvey C, Johnstone R, Anderson E (2000) Understanding the resistivities observed in geothermal systems. In: proceedings world geothermal congress, Kyushu-Tohoku, Japan, pp 1915–1920
Volpi G, Manzella A, Fiordelisi A (2003) Investigation of geothermal structures by magnetotellurics (MT): an example from the Mt. Amiata area, Italy. Geothermics 32:131–145
Wannamaker PE (1997a) CSAMT survey over the sulphur springs thermal area, Valles Caldera, New Mexico, USA, Part I: implications for structure of the western caldera. Geophysics 62:451–465
Wannamaker PE (1997b) Tensor CSAMT survey over the sulphur springs thermal area, Valles Caldera, New Mexico, USA, Part II: implications for CSAMT methodology. Geophysics 62:466–476
Wannamaker PE, Rose PE, Doerner WM, Berard BC, McCulloch J, Nurse K (2004) Magnetotelluric surveying and monitoring at the Coso geothermal area, California, in support of the enhanced geothermal systems concept: survey parameters and initial results. In: proceedings, 29th workshop on geothermal reservoir Engineering, Stanford University
Wannamaker PE, Doerner WM, Hasterok DP (2007) Integrated dense array and transect MT surveying at dixie valley geothermal area, Nevada; structural controls, hydrothermal alteration and deep fluid sources. In: proceedings, 32th workshop on geothermal reservoir Engineering, Stanford University
Wright PM, Ward SH, Ross HP, West RC (1985) State of the art geophysical exploration for geothermal resources. Geophysics 50:2666–2696
Yamane K, Ohsato K, Ohminato T, Kim HJ (2000) Three-dimensional magnetotelluric investigation in Kakkonda geothermal area, Japan. In: proceedings world geothemal congress, Tohoku-Kyushu, Japan, pp 1965–1968
Yu G, Strack K, Tulinius H, Þorbergsóttir IM Ádám L, Hu ZZ, He ZX (2010) Integrated MT/Gravity geothermal exploration in Hungary: A success story. 21 ASEG Conference and Exhibition, Sydney